Journal of Neurochemistry

JNC

JOURNAL OF NEUROCHEMISTRY | 2017

doi: 10.1111/jnc.14146

ORIGINAL ARTICLE

Role of the GM1 ganglioside oligosaccharide portion in the TrkA-dependent neurite sprouting in neuroblastoma cells

Elena Chiricozzi,*,[1] Diego Yuri Pomè,*,[1] Margherita Maggioni,* Erika Di Biase,* Chiara Parravicini,† Luca Palazzolo,† Nicoletta Loberto,* Ivano Eberini† and Sandro Sonnino*

*Department of Medical Biotechnology and Translational Medicine, University of Milano, Segrate, Milano, Italy

†Department of Pharmacological and Biomolecular Sciences, University of Milano, Milano, Italy

Abstract

GM1 ganglioside (II^3NeuAc-Gg_4Cer) is known to promote neurite formation in neuroblastoma cells by activating TrkA-MAPK pathway. The molecular mechanism by which GM1 is involved in the neurodifferentiation process is still unknown, however, *in vitro* and *in vivo* evidences have suggested that the oligosaccharide portion of this ganglioside could be involved. Here, we report that, similarly to the entire GM1 molecule, its oligosaccharide II^3NeuAc-Gg_4, rather than its ceramide (Cer) portion is responsible for the neurodifferentiation process by augmenting neurite elongation and increasing the neurofilament protein expression in murine neuroblastoma cells, Neuro2a. Conversely, asialo-GM1, GM2 and GM3 oligosaccharides are not effective in neurite elongation on Neuro2a cells, whereas the effect exerted by the Fuc-GM1 oligosaccharide ($IV^2\alpha Fuc II^3$Neu5Ac-Gg_4) is similar to that exerted by GM1 oligosaccharide. The neurotrophic properties of GM1 oligosaccharide are exerted by activating the TrkA receptor and the following phosphorylation cascade. By photolabeling experiments performed with a nitrophenylazide containing GM1 oligosaccharide, labeled with tritium, we showed a direct interaction between the GM1 oligosaccharide and the extracellular domain of TrkA receptor. Moreover, molecular docking analyses confirmed that GM1 oligosaccharide binds the TrkA-nerve growth factor complex leading to a binding free energy of approx. −11.5 kcal/mol, acting as a bridge able to increase and stabilize the TrkA-nerve growth factor molecular interactions.

Keywords: differentiation, GM1 ganglioside, GM1 oligosaccharide chain, neuronal development, plasma membrane signaling, TrkA neurotrophin receptor.

J. Neurochem. (2017) https://doi.org/10.1111/jnc.14146

Gangliosides, glycosphingolipids containing sialic acid, constitute a wide family whose components differ in the structure of both the oligosaccharide and lipid chains (Sonnino *et al.* 2006). They are typical components of neuronal membranes taking place with a 10-fold higher amount than in non-neuronal cells and presenting oligosaccharide chains that contain up to five residues of sialic acid. Their change in concentration during brain development suggests specific roles in the nervous system (Allende and

Received May 24, 2017; revised manuscript received July 12, 2017; accepted August 2, 2017.

Address correspondence and reprint requests to Prof. Sandro Sonnino, Via Fratelli Cervi 93, 20090 Segrate (MI), Italy. E-mail: sandro.sonnino@unimi.it

[1]These authors contributed equally to this work.

Ganglioside nomenclature is in accordance with IUPAC-IUBB recommendations (IUPAC-IUMBMB 1998).

Abbreviations used: AGM1, tetrahexosylceramideGg_4; DMEM, Dulbecco's modified Eagles' medium; ERK1/2, extracellular signal-regulated protein kinases 1 and 2; FBS, fetal bovine serum; Fucosylated GM1 oligosaccharide, $IV^2\alpha Fuc II^3$Neu5Ac-Gg_4; GM1 oligosaccharide, II^3Neu5Ac-Gg_4; GM1, II^3Neu5Ac-Gg_4Cer, β-Gal-(1-3)-β-GalNAc-(1-4)-[α-Neu5Ac-(2-3)]-β-Gal-(1-4)-β-Glc-Cer; GM2 oligosaccharide, II^3Neu5Ac-Gg_3; GM3 oligosaccharide, sialyllactose; HPTLC, high-performance silica gel thin-layer chromatography; MAPK, mitogen-activated protein kinase; MTT, 3-(4,5,-dimethylthiazole-2yl)-2,5-diphenyltetrazolium bromide; N2a, Neuro2a cells; NF, neurofilament; NGF, nerve growth factor; PBS, phosphate-buffered saline; p-ERK1/2, phosphorylated ERK1/2; PM, plasma membrane; p-TrkA, phosphorylated TrkA; PVDF, polyvinylidene difluoride; siRNA, short interfering RNA; Trk, neurotrophin tyrosin kinase receptor; Tyr490, tyrosine 490; α-tub, α-tubulin.

Panzetta 1994; Wu *et al.* 1995; Kwak *et al.* 2005; Yu *et al.* 2009; Aureli *et al.* 2011). Particular attention has been devoted to ganglioside GM1, II^3NeuAc-Gg_4Cer (Ledeen and Wu 2015; Schengrund 2015; Aureli *et al.* 2016), structurally characterized by the oligosaccharide chain II^3NeuAc-Gg_4, β-Gal-(1-3)-β-GalNAc-(1-4)-[α-Neu5Ac-(2-3)]-β-Gal-(1-4)-β-Glc- (Kuhn and Wiegandt 1963). *In vitro* and *in vivo* approaches highlighted the neurotrophic and neurodifferentiative functions of ganglioside GM1 (Roisen *et al.* 1981; Facci *et al.* 1984; Chigorno *et al.* 1985; Lipartiti *et al.* 1991; Rodriguez *et al.* 2001; Da Silva *et al.* 2005; Mocchetti 2005; Schneider *et al.* 2010; Sonnino *et al.* 2011; Miyagi and Yamaguchi 2012). The effects exerted by GM1 occur when its plasma membrane (PM) content increases in membrane lipid micro-domains (Hakomori *et al.* 1998). The membrane local enrichment causes (i) the GM1 content-dependent membrane reorganization, which alters membrane properties and ensures the physical parameters required for proper protein function or (ii) the GM1 oligosaccharide–protein direct interactions, which modify the protein conformation and function (Coskun and Simons 2011).

The plasma membrane increase of GM1 is responsible for the activities of several membrane enzyme and receptor (Tettamanti 1986; Zoli *et al.* 1990). In fact, membrane-associated proteins, including neurotrophin receptors, opioid receptors, integrins and calcium transporter, have been proposed as interactor partners of GM1 (Ledeen and Wu 2015). In particular, interaction between GM1 and the neurotrophin tyrosin kinase receptor (Trk) has been claimed for modulation of neuritogenesis (Ferrari *et al.* 1995; Mutoh *et al.* 1995; Farooqui *et al.* 1997; Bachis *et al.* 2002). As described by different authors, plasma membrane increase of GM1 and formation of a GM1 enriched platform leads to membrane reorganization triggering to the dimerization of TrK, followed by its autophosphorylation (Rodriguez *et al.* 2001; Da Silva *et al.* 2005).

In spite of many papers, connect the neurite elongation with GM1 plasma membrane content and with modulation of the Trk activity, the precise GM1 mechanism of action remains elusive. Opposite experimental approaches, such as the PM sialidase NEU3 over-expression, but also its inhibition, led to think that changes in oligosaccharidic chains of plasma membrane gangliosides could affect the fine tuning of the processes through the plasma membrane (Rodriguez *et al.* 2001; Valperta *et al.* 2007). However, only few data concerning the relationship between ganglioside oligosaccharide and neuritogenesis processes have been reported so far (Schengrund and Prouty 1988). For this reason, we decided to investigate the role played by the oligosaccharide chain of GM1 and we found out that the GM1 oligosaccharide is able to promote the TrkA-dependent neurite sprouting in mouse neuroblastoma cells.

Methods

Materials

Commercial chemicals were of the highest purity available, common solvents were distilled before use and water was doubly distilled in a glass apparatus.

Cell culture plates and Transfectagro™ reduced serum medium were from Corning (Corning, NY, USA). Mouse neuroblastoma Neuro2a (N2a) cells (RRID: CVCL_0470), phosphate-buffered saline (PBS), Paraformaldehyde, Triton X-100, sodium dodecyl sulfate (SDS), 2-propanol, Formic acid, 3-(4,5,-dimethylthiazole-2yl)-2,5-diphenyltetrazolium bromide (MTT), Trypan blue, Galactose, Sialic Acid, anti-rabbit FITC conjugate, and mouse α-tubulin antibodies were from Sigma-Aldrich (St. Louis, MO, USA). Dulbecco's modified Eagle's high glucose medium, fetal bovine serum (FBS), L-glutamine (L-Glut), Penicillin (10.000 U/mL), Streptomycin and 30% acrylamide were from EuroClone (Paignton, UK). Gibco™ OptiMEM™ I reduced serum medium, Lipofectamine® 2000 and goat anti-mouse IgG (H+L) antibody (RRID: AB_228307) were from Thermo Fischer Scientific (Waltham, MA, USA). TrkA inhibitor (CAS 388626-12-8) was from Merk Millipore (Billerica, MA, USA). The short interfering RNAs (siRNAs) were from Quiagen (Velno, Netherlands). Rabbit anti-TrkA (RRID: AB_10695253), rabbit anti-phospho-TrkA (tyrosine 490, Tyr490) (RRID: AB_10235585), rabbit anti-p44/42 MAPK (Erk1/2) (RRID: AB_390779), rabbit anti-phospho-p44/42 MAPK (pErk1/2) (Thr202/Tyr204) (RRID: AB_2315112) and anti-rabbit IgG (RRID: AB_2099233) antibodies were from Cell Signaling Technology (Danvers, MA, USA). Rabbit anti-pan Neurofilament (NF) antibody (RRID: AB_10539699) was from Biomol International (Plymouth Meeting, PA, USA). Chemiluminescent kit for western blot was from Cyanagen (Bologna, Italy). Ultima gold was from Perkin Elmer (Waltham, MA, USA). DC protein assay kit was from BioRad (Hercules, CA, USA). High-performance thin-layer chromatography (HPTLC) was from Merk Millipore (Frankfurten, Germany). Polyvinylidene difluoride (PVDF) membrane was from GE Healthcare Life Sciences (Chigago, IL, USA).

Preparation of gangliosides and their oligosaccharides

Fuc-GM1 (Ghidoni *et al.* 1976), GM1 and GM2 gangliosides were purified from the total ganglioside mixture extracted from pig brains (Tettamanti *et al.* 1973), submitted to sialidase hydrolysis (Acquotti *et al.* 1994). Desialylated GM1 (AGM1, asialo-GM1) was prepared by acid hydrolysis of GM1 and chromatographic purification (Ghidoni *et al.* 1976). GM1 containing tritium at position 6 of external galactose was prepared by enzymatic oxidation with galactose oxidase followed by reduction with sodium boro[^{3}H]hydride (Sonnino *et al.* 1996). The oligosaccharides Gg_4, II^3Neu5Ac-Lac, II^3Neu5Ac-Gg_3, II^3Neu5Ac-[^{3}H]Gg_3, II^3Neu5Ac-Gg_4, II^3Neu5Ac-[^{3}H]Gg_4, and IV^2αFucII^3-Neu5Ac-Gg_4, were prepared by ozonolysis followed by alkaline degradation (Wiegandt and Bucking 1970), from tetrahexosylceramide, GM3, GM2, [^{3}H]GM2, GM1, [^{3}H]GM1, and Fuc-GM1, respectively. Altogether, NMR, MS, HPTLC, and autoradiographic analyses showed a homogeneity over 99% for all the prepared gangliosides and oligosaccharides (data not shown).

Tritium-labeled and photoactivable GM1 oligosaccharide, II^3Neu5Ac-[^{3}H]Gg_4-N_3, was prepared from II^3Neu5Ac-[^{3}H]Gg_4, according to the scheme reported in Fig. 1.

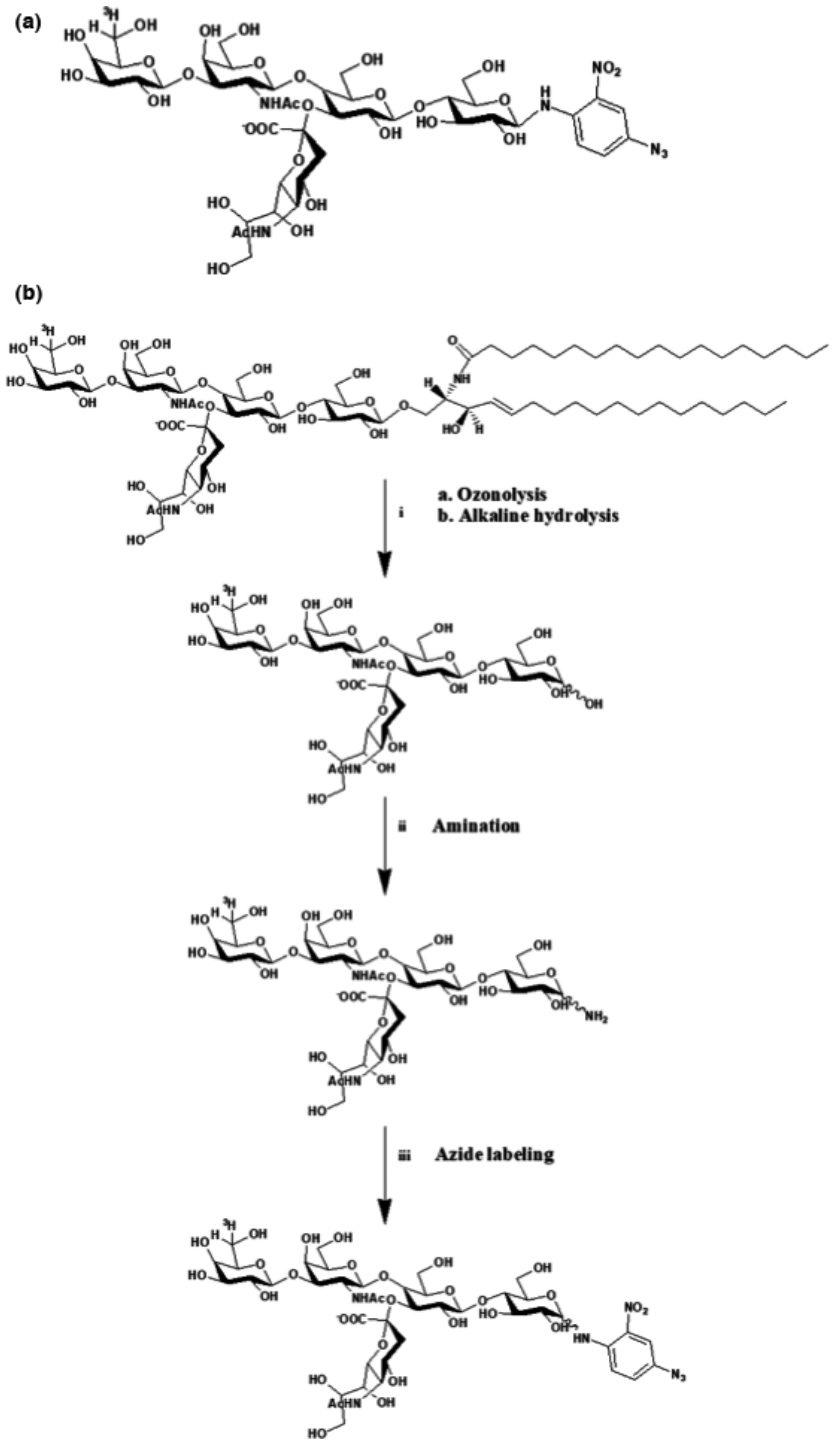

Fig. 1 $II^3Neu5Ac\text{-}[^3H]Gg_4\text{-}N_3$ structure and chemical synthesis. (a) Structure of $II^3Neu5Ac\text{-}[^3H]Gg_4\text{-}N_3$. (b) Scheme of the synthetic process for the preparation of $II^3Neu5Ac\text{-}[^3H]Gg_4\text{-}N_3$. Reagents and conditions: (i) a. O_3, CH_3OH, 23°C, 30 min.; (b) triethylamine, 23°C, 18 h; (ii) NH_4HCO_3, NH_4OH 33%, 40°C, 48 h; (iii) 2-nitro-4-fluorophenylazide, Bu_3N, DMF/dimethylsulfoxide, 80°C, 18 h. Final yield, 45%.

An amount of 52 μmoles of $II^3Neu5Ac\text{-}[^3H]Gg_4$ (0.5 Ci/mmol) were dissolved in 33% ammonia and treated with 1 mg of ammonium hydrogen carbonate. The reaction was maintained under stirring for 48 h at 40°C. The solution was then immediately freeze-dried (Lubineau *et al.* 1995).

The crude amino-$II^3Neu5Ac\text{-}[^3H]Gg_4$ was dissolved in 0.5 mL of dry dimethylformamide, then 1 mg of 2-nitro-4-fluorophenylazide and 1 μL of tributylamine in 25 μL of dry dimethylsulfoxide were added under dark conditions. Maintaining dark conditions for all the process, the reaction mixture was stirred overnight at 80°C. After solvent evaporation, the photoactivable $II^3Neu5Ac\text{-}[^3H]Gg_4\text{-}N_3$ was purified by flash chromatography using chloroform/methanol/2-propanol/water 60 : 35 : 5 : 5 as eluent (Mauri *et al.* 2004). $II^3Neu5Ac\text{-}[^3H]Gg_4\text{-}N_3$ solubilized in methanol was stored at 4°C.

HPTLC analyses were performed using the solvent system chloroform/methanol/0.2% $CaCl_2$, 60 : 35 : 8 by vol. Bound sialic acid was determined by the resorcinol-HCl method (Svennerholm 1957; Takki-Luukkainen and Miettinen 1959), pure Neu5Ac being used as the reference standard.

Cell cultures

N2a cells were cultured and propagated as monolayer in Dulbecco's modified Eagle's medium-High Glucose medium supplemented with 10% heat inactivated FBS, 1% L-glutamine and 1% penicillin/streptomycin, at 37°C in a humidified atmosphere of 95% air/5% CO_2. Cells were subcultured to a fresh culture when growth reached the 80–90% confluence (i.e. every 3–4 days).

Cell treatments

N2a cells were plated at $5 \times 10^3/cm^2$ and incubated for 24 h to allow cells attachment and recovery in complete medium before all treatments. Control cells were incubated under identical conditions but omitting any addition.

Ganglioside and oligosaccharide treatments

To induce differentiation, growth medium was removed and cells were pre-incubated in pre-warmed (37°C) Transfectagro medium containing 2% FBS, 1% L-glutamine, 1% penicillin/streptomycin, for 30 min at 37°C. Cell treatments were performed in serum reduced culture medium, in order to minimize interactions between serum components and exogenous gangliosides or their oligosaccharides. Subsequently, cells were incubated at 37°C up to 48 h in the presence of 50 μM gangliosides, oligosaccharides, galactose, or sialic acid.

TrkA chemical inhibition experiments

In order to block TrkA activity in N2a cells, the TrkA inhibitor (120 nM) was added to the incubation medium 1 h before the addition of GM1 or $II^3Neu5Ac\text{-}Gg_4$ (Wood *et al.* 2004).

siRNA mediated RNA interference experiments

TrkA knockdown was achieved by RNA interference applying siRNA. Three distinct siRNAs were used to silence TrkA: Mm_Ntrk1_1 (sense 5′-CCAUCAUAAUAGCAAUUAUTT-3′, antisense 5′-AUAAUUG CUAUUAUGGAT-3′); Mm_Ntrk1_5 (sense 5′-GGUGGCUGCUG GUAUGGUATT-3′, antisense 5′-UACCAUACCAGCAGCCACC TG-3′); and Mm_Ntrk1_6 (sense 5′-CCUUCUUGUGCUCAA CAAATT-3′, antisense 5′-UUUGUUGAGCACAAGAAGGAG-3′). As a negative control, non-silencing siRNA with no homology to any known mammalian gene was used (sense 5′-UUCUUCGAACGUGU CACGUdTdT-3′, antisense 5′-ACGUGACACGUUCGGAGAA dTdT-3′). Transfection was performed after 24 h from cell plating in antibiotic and serum free culture media with solution containing 25% OptiMEM, 0.25% Lipofectamine 2000 and 50 nM siRNA (16.7 nM of each siRNA). After 6 h, the transfection medium was changed to culture medium containing antibiotic and serum. After 24 h from the silencing, cells were treated with GM1 or $II^3Neu5Ac\text{-}Gg_4$ as above.

Photolabeling experiments

Cells were incubated with 50 μM $II^3Neu5Ac\text{-}[^3H]Gg_4\text{-}N_3$ for 3 h at 37°C. After incubation, medium was removed and cells were illuminated for 40 min under UV light (λ = 360 nm) on ice to induce photo-activation. All the procedures before exposure to UV light were performed under red safelight. The cells were lyzed and subjected to 4–20% sodium dodecyl sulfate–polyacrylamide gel electrophoresis (SDS–PAGE) and blotted on PVDF membrane. Digital autoradiography of the PVDF membrane was performed with Beta-Imager 2000 (Biospace, Paris, France). PVDF membrane was then incubated with anti-TrkA antibody (Sonnino *et al.* 1989, 1992; Chigorno *et al.* 1990; Loberto *et al.* 2003; Chiricozzi *et al.* 2015).

Determination of cell viability

Cell viability was determined by Trypan blue exclusion and by MTT assays after 12, 24 and 48 h treatment with gangliosides and oligosaccharides. The number of living and death cells has been determined by counting cells after Trypan blue staining, as previously described (Mehlen *et al.* 1988; Aureli *et al.* 2011). Proliferation was determined by the MTT method (Mosmann 1983). Briefly, at the end of incubation, 2.4 mM MTT (4 mg/mL in PBS) were added to each well and plates were re-incubated for 4 h at 37°C. Medium was carefully removed and replaced with 2-propanol: formic acid, 95 : 5 (v/v). Plates were gently agitated prior to read the absorbance at 570 nm with a microplate spectrophotometer (Wallac 1420 VICTOR2™; Perkin Elmer).

Morphological analysis and neurite outgrowth evaluation

Cultured cells treated with ganglioside GM1 or different oligosaccharides were observed by phase contrast microscopy (Olympus BX50 microscope; Olympus, Tokyo, Japan). The neurite-like length was measured on bidimensional images and expressed as the ratio between neurite length and cell body diameter (Schengrund and Prouty 1988). Five random fields were examined from each well, giving a total cell count of at least 200 cells per well.

Immunofluorescence analysis

Treated or not treated cells were fixed in 4% paraformaldehyde for 20 min at 23°C. Cells were permeabilized with 0.1% Triton X-100 for 30 min and then treated with a blocking solution for 1 h at 23°C. Cells were incubated with rabbit polyclonal antibody anti-NF for 2 h at 23°C. After washing with PBS, cells were incubated 1 h with secondary anti-rabbit antibody FITC-conjugated. Fluorescence microscopy was carried out using an Olympus U-RFL-T EPI Fluorescence Microscope (Olympus) and the images processing were performed with ImageJ software.

Fate of $II^3Neu5Ac\text{-}Gg_4$ added to the cells

Fate of $II^3Neu5Ac\text{-}Gg_4$ administered to cells was determined using tritium-labeled $II^3Neu5Ac\text{-}Gg_4$. After the cell administration with 50 μM $II^3Neu5Ac\text{-}[^3H]Gg_4$ for different times, the medium was removed and the following treatments were performed sequentially: (i) cells were washed five times with 10% FBS-medium to remove the amount of $II^3Neu5Ac\text{-}Gg_4$ weakly associated to the cells — serum removable fraction; (ii) cells were treated with 0.1% trypsin solution to evaluate the $II^3Neu5Ac\text{-}Gg_4$ strongly linked to extracellular domain of PM proteins — trypsin removable fraction; (iii) cells were lyzed in order to evaluate the quantity of $II^3Neu5Ac\text{-}Gg_4$ internalized — trypsin stable fraction. The procedure was established previously to determine the fate of gangliosides administered to cells in culture (Chigorno *et al.* 1985).

Protein analysis

Equal amounts of proteins derived from treated and untreated cells were denatured, separated on 7.5% polyacrylamide gels, and transferred to PVDF membranes. The presence of NF, TrkA, p-TrkA, extracellular signal-regulated protein kinases 1 and 2 (ERK1/2) and p-ERK1/2 was determined by specific primary antibodies, followed by reaction with secondary horseradish peroxidase-conjugated antibodies. α-tubulin was used as loading control. The data acquisition and analysis were performed using Alliance Uvitec (Eppendorf, Germany).

Molecular modeling

Crystallographic structure of the extracellular segment of human TrkA in complex with nerve growth factor (NGF) (RCSB PDB ID: 2IFG) was used for molecular docking calculations. Protein complex was submitted to the Molecular Operating Environment 2016.0802 (MOE) Structure Preparation application, in order to fix all issues and to prepare structures for subsequent computational analyses.

The $II^3Neu5Ac\text{-}Gg_4$ structure was built with the MOE Carbohydrate Builder and a geometry optimization was carried out with MOPAC7 and the PM6 basis set.

Molecular docking was carried out through the MOE Dock program, setting as receptor the complex between TrkA and NGF, as ligand the optimized $II^3Neu5Ac\text{-}Gg_4$ structure. The binding site was identified at the interface between the two proteins. Before placement procedure, 20 000 rotamers of the ligand was generated, exploring all the molecule rotatable bonds. Alpha PMI placement algorithm, specifically developed for tight binding pocket, was selected. The London dG empirical scoring function was used for sorting the poses. The 30 top-scoring poses was refined through molecular mechanics, considering the receptor as a rigid body, and the refined complexes were scored through the GBVI/WSA dG empirical scoring function, keeping the five top-scoring poses.

The top-scoring pose from the docking procedure was refined by using the MOE QuickPrep procedure aimed at relaxing and refining the complex before calculating the approx. binding free energy *via* the GBVI/WSA dG empirical scoring function (Naim *et al.* 2007).

Statistical analysis

Data are expressed as mean ± SEM and were analyzed for significance by Student's *t*-test or two-way ANOVA test. The analysis was performed with Prism software (GraphPad Software, Inc. La Jolla, CA, USA).

Other analytical methods

NMR spectra were recorded with a Bruker AVANCE-500 spectrometer at a sample temperature of 298 K. NMR spectra were recorded in CDCl3 or CD3OD and calibrate using the TMS signal as internal reference.

Mass spectrometric analysis were performed in positive or negative ESI-MS. MS spectra were recorded on a Thermo Quest Finningan LCQTM DECA ion trap mass spectrometer, equipped with a Finnigan ESI interface; data were processed by Finnigan Xcalibur software system (Thermo Fischer Scientific, Waltham, MA, USA).

All reactions were monitored by TLC on silica gel 60 plates (Merck).

Radioactivity associated with cells and trypsin and serum labile cell fractions was determined by liquid scintillation counting. Digital autoradiography of the PVDF membranes was performed with a Beta-Imager 2000 (Biospace).

Any randomization or blinding procedures were performed for our experiments. Institutional approval was not needed.

Results

N2a cell viability upon treatments with ganglioside GM1 and its oligosaccharide

Trypan blue assay, performed on N2a cells treated with 50 μM GM1 ganglioside or its oligosaccharide up to 48 h, showed a viability overlapping to that of control cells and over 94% (Fig. 2a). On the other hand, we observed a reduction in cell proliferation starting from 12 h of treatment (Fig. 2b).

Neurite sprouting by administration to N2a cells of $II^3Neu5Ac\text{-}Gg_4$

Incubation of N2a cells with $II^3Neu5Ac\text{-}Gg_4$ induced a neuron-like morphology after 24 (Fig. 3) and 48 h (Figure S1), pointing out the sprouting and elongation of neurites, which are almost absent in round-shaped control cells. A similar result was obtained in cells treated with GM1, confirming previous data (Facci *et al.* 1984; Rabin *et al.*

(a)

	Cell viability (%)		
	h 0	h 24	h 48
Untreated cells	96 ± 2	94 ± 1	94 ± 2
+ GM1	94 ± 2	94 ± 2	94 ± 1
+ $II^3Neu5Ac\text{-}Gg_4$	96 ± 1	94 ± 2	95 ± 2

(b)

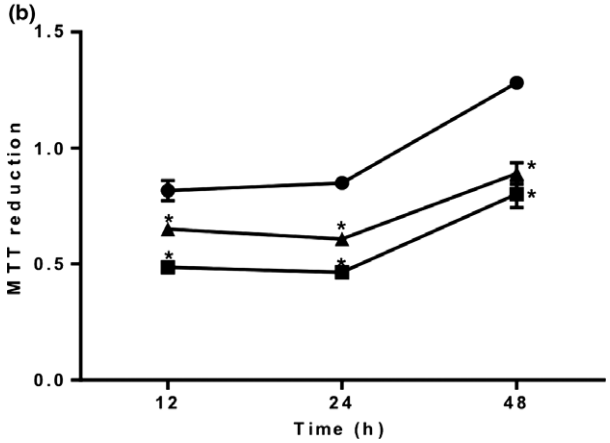

Fig. 2 Effect of GM1 and $II^3Neu5Ac\text{-}Gg_4$ on Neuro2a (N2a) cell viability. N2a cells were induced to differentiate in the presence or absence of 50 μM GM1 or $II^3Neu5Ac\text{-}Gg_4$ up to 48 h. (a) The number of living and death cells was determined by Trypan blue exclusion assay. Values represent the percentage mean of living cells ± SEM for three different culture preparations ($n = 3$). (b) Cell proliferation was evaluated by 3-(4,5,-dimethylthiazole-2yl)-2,5-diphenyltetrazolium bromide (MTT) reduction assay on N2a cells grown in the absence (●) or presence of GM1 (□) or $II^3Neu5Ac\text{-}Gg_4$ (▲). Results are expressed as mean of absorbance values at 570 nm ± SEM for three different culture preparations (*$p < 0.05$ vs. CTRL, two-way ANOVA, $n = 3$).

2002). N2a cells were treated with Gg_4, $II^3Neu5Ac\text{-}Gg_3$, sialyllactose, galactose, or sialic acid in order to clarify the minimal structure required to promote neurite elongation. None of these compounds induced cell morphological changes (Fig. 3 and Figure S1), suggesting that the whole structure of the $II^3Neu5Ac\text{-}Gg_4$ is necessary to block cell proliferation and to induce neurite sprouting. In addition, cells were treated with fucosylated $II^3Neu5Ac\text{-}Gg_4$, which induces neurite sprouting and reduction of cell proliferation in a similar way as $II^3Neu5Ac\text{-}Gg_4$. This result suggests that the neurite sprouting process requires specifically the β-Gal-(1-3)-β-GalNAc-(1-4)-[α-Neu5Ac-(2-3)]-β-Gal-(1-4)-Glc structure and that the addition to it of an α-fucose at position 2 of the external galactose is irrelevant for the processes (Fig. 3 and Figure S1).

Neurite extensions, observed after 24 h treatment with $II^3Neu5Ac\text{-}Gg_4$, were measured as the ratio between the length of processes and the diameter of cell body (Fig. 4a). This ratio resulted at least two fold higher compared to the control and similar to GM1-treated cells.

Expression of heavy, medium, and light intracellular NF subunits (NF-H, NF-M and NF-L), considered markers of neurodifferentiation (Fukuda *et al.* 2014), was evaluated by immunoblotting. NF proteins are considered the major components of cytoskeleton supporting axonal construction. NF expression increased significantly after 24 h treatment with both GM1 and $II^3Neu5Ac\text{-}Gg_4$ (Fig. 4b), resulting quite evident by immunofluorescence (Fig. 4c).

Fate of the $II^3Neu5Ac\text{-}Gg_4$ added to N2a cells

Isotopic tritium-labeled $II^3Neu5Ac\text{-}Gg_4$ was administered to the N2a cells. After 0.5, 1, 6, and 24 h treatment, cells were treated according to a procedure previously developed (Chigorno *et al.* 1985). At the end of the incubation, cells were washed with culture medium containing 10% serum in order to evaluate the quantity of oligosaccharide weakly associated to the cells surface (serum labile). Successively cells were treated with trypsin to evaluate a possible portion strongly bond to the extracellular domain of PM proteins (trypsin labile). At the end, cells were lyzed in order to evaluate the quantity of internalized $II^3Neu5Ac\text{-}Gg_4$ (trypsin stabile). At each time point analyzed, about 99% of $II^3Neu5Ac\text{-}Gg_4$ was found in the serum labile form as shown in Fig. 5. This suggests that the $II^3Neu5Ac\text{-}Gg_4$ is not taken up by the cells and that it is associated to PM proteins.

TrkA-dependent neuritogenesis induced by $II^3Neu5Ac\text{-}Gg_4$

It was previously reported that GM1 promotes neurite elongation by amplifying the effect exerted by NGF on TrkA (Farooqui *et al.* 1997; Singleton *et al.* 2000; Duchemin *et al.* 2002; Da Silva *et al.* 2005; Mocchetti 2005; Zakharova *et al.* 2014). We checked the activation of TrkA receptor in N2a cells treated with the $II^3Neu5Ac\text{-}Gg_4$, to verify the role of $II^3Neu5Ac\text{-}Gg_4$ in the GM1-promoted TrkA activation. In detail, we focused on phosphorylation of Tyr490, which leads to the activation of the neuronal differentiation pathway (Singleton *et al.* 2000; Duchemin *et al.* 2002; Huang and Reichardt 2003; Zakharova *et al.* 2014). By immunoblotting analysis, we highlighted the activation of TrkA receptor revealed by the increase in the phosphorylation of Tyr490 either in GM1-treated cells and in cells that received $II^3Neu5Ac\text{-}Gg_4$ (Fig. 6a). In the treated cells, we also checked the activation of MAP kinases founding an increase of ERK1/2 phosphorylation (Fig. 6a). To prove that the neuritogenic effect exerted by the GM1 or its oligosaccharide was directly mediated by TrkA-ERK pathway, we blocked the TrkA receptor by chemical inhibition, using a specific TrkA inhibitor, able to fit in the ATP pocket (Wood *et al.* 2004). The addition of TrkA inhibitor together with the GM1 or the $II^3Neu5Ac\text{-}Gg_4$ prevented the phosphorylation processes (Fig. 6a) and the neurite elongation (Fig 6b).

Furthermore, to prove the necessary requirement of TrkA in $II^3Neu5Ac\text{-}Gg_4$-mediated neuritogenesis, TrkA was knocked down using the siRNA approach. Control cells were transfected with scramble-siRNA. Silenced cells, resulting in a 70% reduction of TrkA expression (Fig. 7a), were incubated with GM1 or $II^3Neu5Ac\text{-}Gg_4$ for 24 h and no differentiation, nor the phosphorylation of Erk1/2 (Fig. 7b and c) could be observed.

$II^3Neu5Ac\text{-}Gg_4$–TrkA interaction in N2a cells

To study the interaction between the oligosaccharide chain of GM1 and TrkA, we prepared, according to the scheme in Fig. 1, a radioactive and photoactivable $II^3Neu5Ac\text{-}Gg_4$ derivative, $II^3Neu5Ac\text{-}[^3H]Gg_4\text{-}(N_3)$.

N2a cells were incubated with $II^3Neu5Ac\text{-}[^3H]Gg_4\text{-}(N_3)$ under dark conditions. After pulse, cells were illuminated under UV-light to induce covalent cross-linking between cell surface proteins and the radioactive GM1 oligosaccharide derivative. Proteins were separated by SDS–PAGE, blotted on a PVDF membrane and the radioactive bands visualized by digital autoradiography. In comparison to N2a protein pattern, few radioactive bands were detected. They correspond to specific proteins that, after the illumination, are covalently bond with $II^3Neu5Ac\text{-}Gg_4$ (Fig. 8). After radioimaging, the PVDF membrane was incubated with TrkA antibody and we could detect a specific TrkA signal co-migrating with the radioactive band at 140 kDa visualized by the digital autoradiography (Fig. 8).

Fig. 3 Effect of GM1, a series of oligosaccharides and saccharides on the morphology of Neuro2a (N2a) cells. N2a cells in the absence (a) or presence of 50 μM galactose (b), sialic acid (c), sialyllactose (d), $II^3Neu5Ac\text{-}Gg_3$ (e), Gg_4 (f), $II^3Neu5Ac\text{-}Gg_4$ (g), $IV^2\alpha FucII^3Neu5Ac\text{-}Gg_4$ (h) and GM1 (i). After 24 h incubation, cells were analyzed with phase contrast microscopy with 200× magnification. Images are representative of ten independent experiments ($n = 10$).

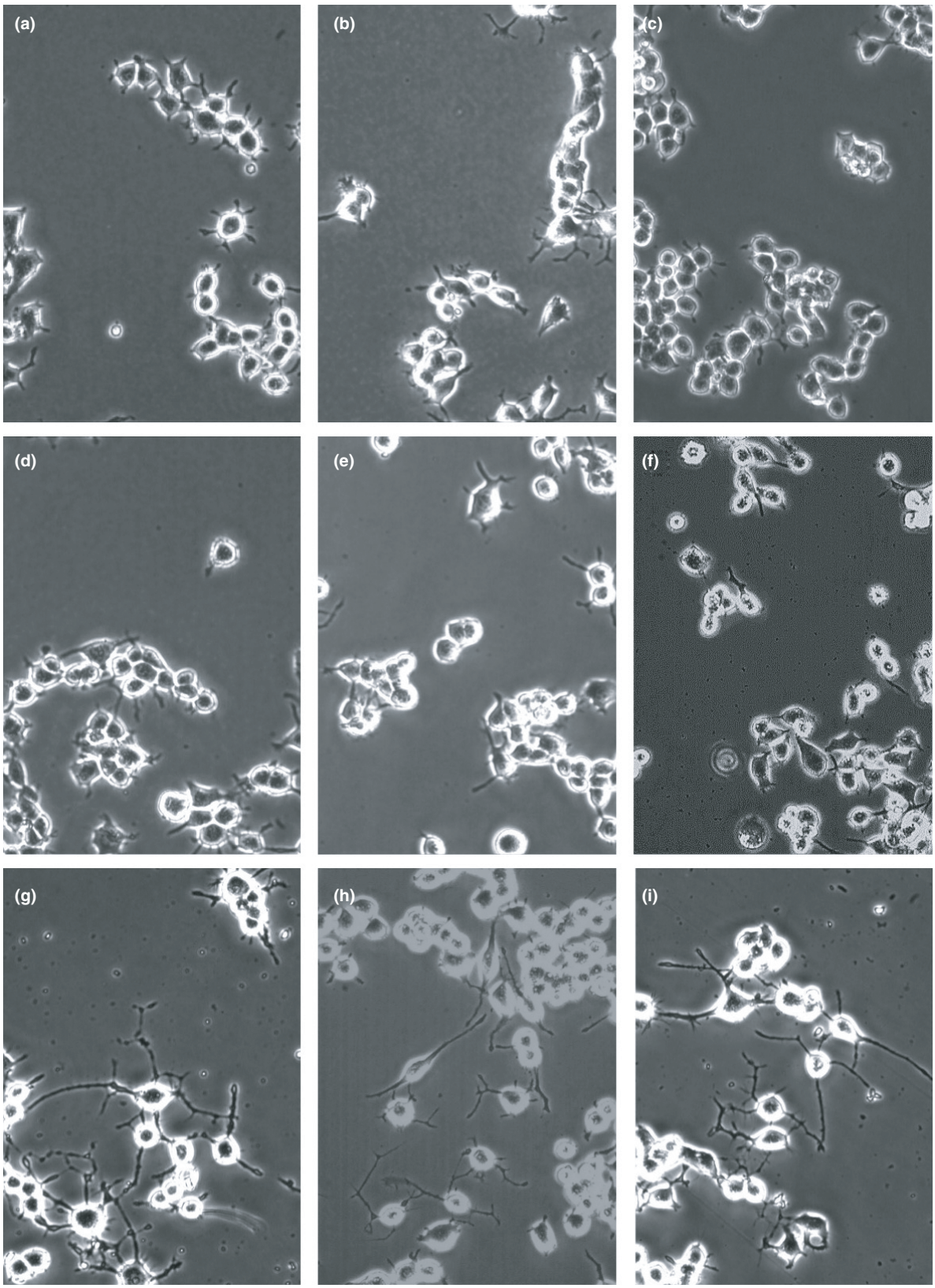

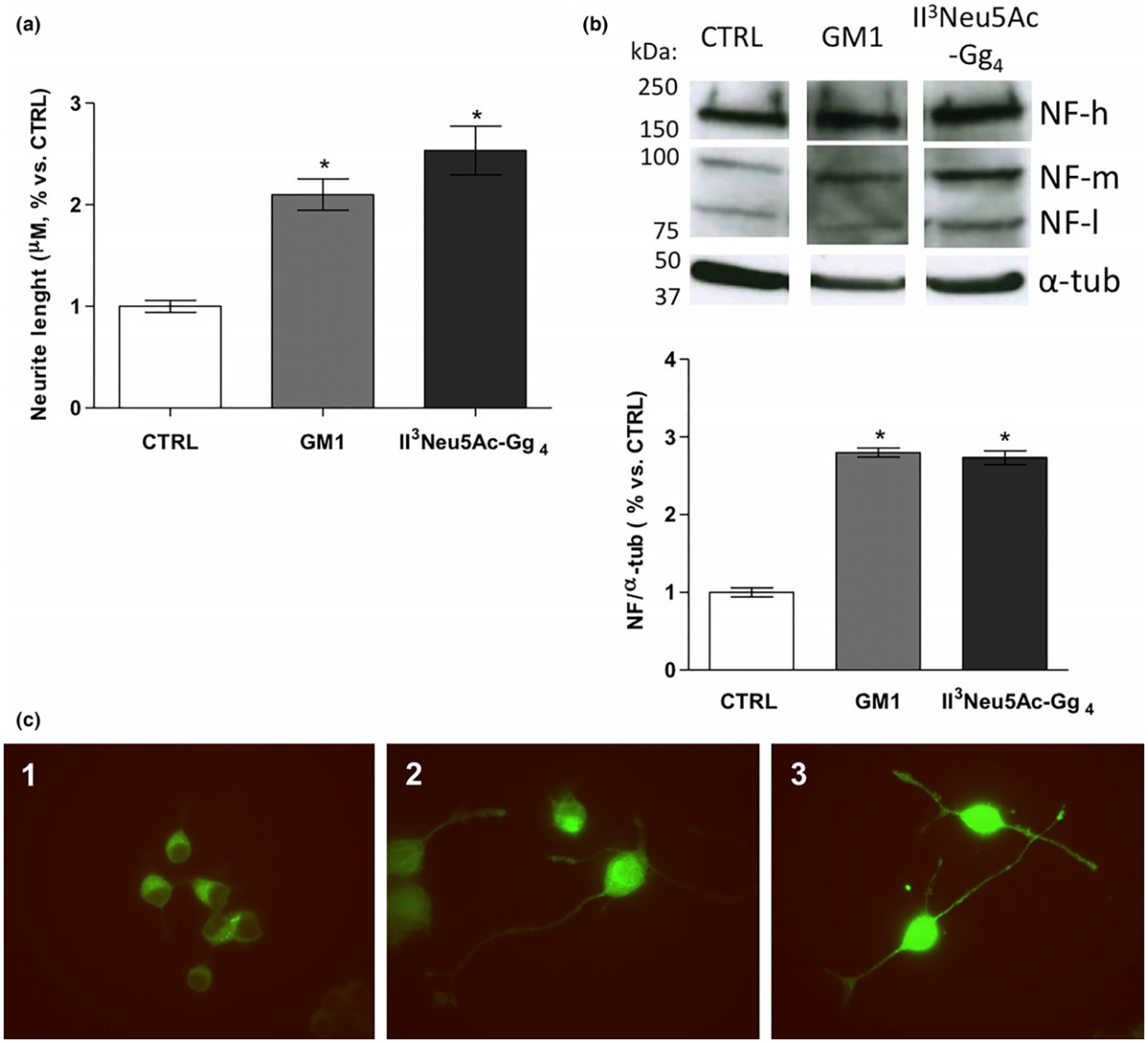

Fig. 4 Characterization of the neurite sprouting in Neuro2a cells following administration of GM1 and II^{3}Neu5Ac-Gg$_4$. (a) Neurite length was measured as the ratio between the length of extensions and cell body diameter. Values are expressed as fold increase over CTRL of mean ± SEM from five different experiments (*$p < 0.01$, Student's *t*-test, $n = 5$); (b) Immunoblotting for neurofilament (NF)-h, NF-m, NF-l expression is revealed by specific antibodies and visualized by chemiluminescence. Top: immunoblotting images. Blots are representative of three independent experiments. Bottom: semi-quantitative analysis of NF proteins amount. α-tubulin (α-tub) was used as internal normalizer. Data are expressed as fold increase over CTRL of mean ± SEM from three different experiments (*$p < 0.01$, Student's *t*-test, $n = 3$); (c) Immunofluorescence staining of NF proteins (400× Magnification), 1, CTRL; 2, GM1; 3, II^{3}Neu5Ac-Gg$_4$. Images are representative of three independent experiments ($n = 3$).

Dynamic calculations for the TrkA-II^{3}Neu5Ac-Gg$_4$ complex

The availability of the crystallographic structure of the extracellular segment of human TrkA in complex with NGF allowed us to support biochemical data with bioinformatics. The molecular docking of II^{3}Neu5Ac-Gg$_4$, specifically carried out exploring the interaction interface between TrkA and NGF, showed that II^{3}Neu5Ac-Gg$_4$ is able to tightly bind both TrkA and NGF contemporarily, producing only one very stable pose, with an approximative binding free energy of −11.3 kcal/mol (Fig. 9).

Discussion

Gangliosides are components of the external layer of plasma membranes where they represent about one-sixth of the total lipid content. In addition to their structural role, they are

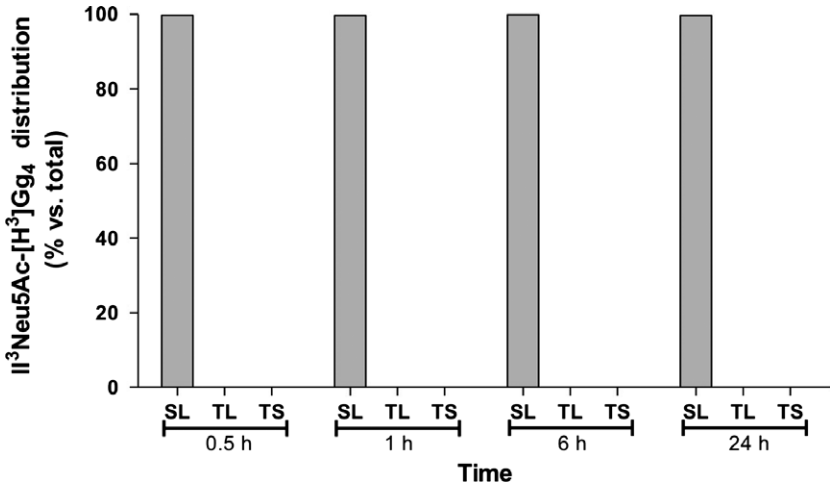

Fig. 5 Association of $II^3Neu5Ac$-[^{3}H]Gg_4 to Neuro2a (N2a) cells. N2a cells were incubated with 50 μM $II^3Neu5Ac$-[^{3}H]Gg_4 for 0.5, 1, 6 and 24 h. After pulse, cells are washed with medium containing 10% fetal bovine serum to obtain the serum labile fraction (SL). Then cells are treated with low concentrated trypsin to obtain the trypsin labile fraction (TL). Finally, cells are lysed to obtain the trypsin stable fraction (TS) corresponding to the fraction of compound taken up by the cells. The radioactivity associated with each fraction was determined by liquid scintillation counting. Data are expressed as percentage mean of total radioactivity ± SEM of three different experiments (n = 3).

considered players in signaling and regulatory pathways. The chemical structure of gangliosides makes them ideal mediators of information across the plasma membrane: the ceramide portion allows hydrophobic interactions inside the membrane core, the ceramide amide linkage leads to the formation of a net of hydrogen bonds at the water–lipid interface and the oligosaccharide facing toward the extracellular environment provides specific side-to-side and head-to-head recognition sites. These properties favor formation of lipid rafts, segregation of proteins and ganglioside–protein interactions, which lead to cell function modulation.

GM1 is the best-studied neuronal ganglioside. Its properties, such as modulation of differentiation, adhesion, migration, neurotrophic factor signaling, axon guidance, synaptic transmission, myelin genesis, and neuron–glia interactions have been described, and continue to be confirmed in several papers (see recent reviews Schengrund 2015; Ledeen and Wu 2015; Aureli *et al.* 2016).

GM1-mediated neurodifferentiation has been studied by *in vitro* and *in vivo* experiments (Facci *et al.* 1984; Lipartiti *et al.* 1991; Rodriguez *et al.* 2001; Da Silva *et al.* 2005; Mocchetti 2005), but the precise molecular mechanism by which GM1 exerts its neurotrophic action is still unclear. Anyhow, the increase of GM1 within the plasma membrane seems to be necessary for TrkA-mediated neurodifferentiative processes; in fact the lack of GM1 caused unresponsiveness of the TrkA protein to NGF (Facci *et al.* 1984; Mutoh *et al.* 1998).

Here, we presented a specific role of GM1 oligosaccharide, a part from the entire ganglioside, in the process of neurite elongation in murine neuroblastoma N2a cells. This line of evidence suggests that ceramide acts as an aglycone, dynamically moving within the membrane layer and allowing different carbohydrate–protein interactions that are dependent on ganglioside content and membrane organization.

For our experiments, we prepared the GM1 oligosaccharide, its tritiated form and its tritiated-and-photoactivable form. The GM1 oligosaccharide was prepared by chemical ozonolysis of pure GM1 followed by alkaline fragmentation according to an old procedure capable to give very high yield (Wiegandt and Bucking 1970). Chromatography and MS analyses showed that the GM1 oligosaccharide was pure and devoid of GM1 (Figure S2). The same procedure was applied to a GM1 carrying tritium at the C6 position of external galactose to obtain $II^3Neu5Ac$-[^{3}H]Gg_4, part of which was derivatized with nitro-phenyl-azide to prepare a tritium-labeled and photoactivable $II^3Neu5Ac$-Gg_4 (Fig. 1).

$II^3Neu5Ac$-Gg_4 was added to cell culture medium to obtain a 50 μM concentration. The $II^3Neu5Ac$-Gg_4 associated to the cell surface could be completely detached from the cells by washing cells with protein solutions (Fig. 5). No detectable amount of $II^3Neu5Ac$-Gg_4 was taken up by the cells. This suggests that the $II^3Neu5Ac$-Gg_4 associated with the surface remains in equilibrium with the free soluble form. The association of $II^3Neu5Ac$-Gg_4 to N2a cells reduced cell proliferation, with no changes in cell viability (Fig. 2), and rapidly produced neurite sprouting (Fig. 3 and Figure S1). The neurite elongation goes together with the increase of neurofilament protein expression (Fig. 4). The neurite sprouting and the expression of neurofilaments are markers of neuronal differentiation (Fukuda *et al.* 2014), and we conclude that the effect exerted by $II^3Neu5Ac$-Gg_4 on N2a cells overlaps to that previously reported for ganglioside GM1 (Facci *et al.* 1984). Moreover, we demonstrated that the effect exerted by $II^3Neu5Ac$-Gg_4 was structure-specific.

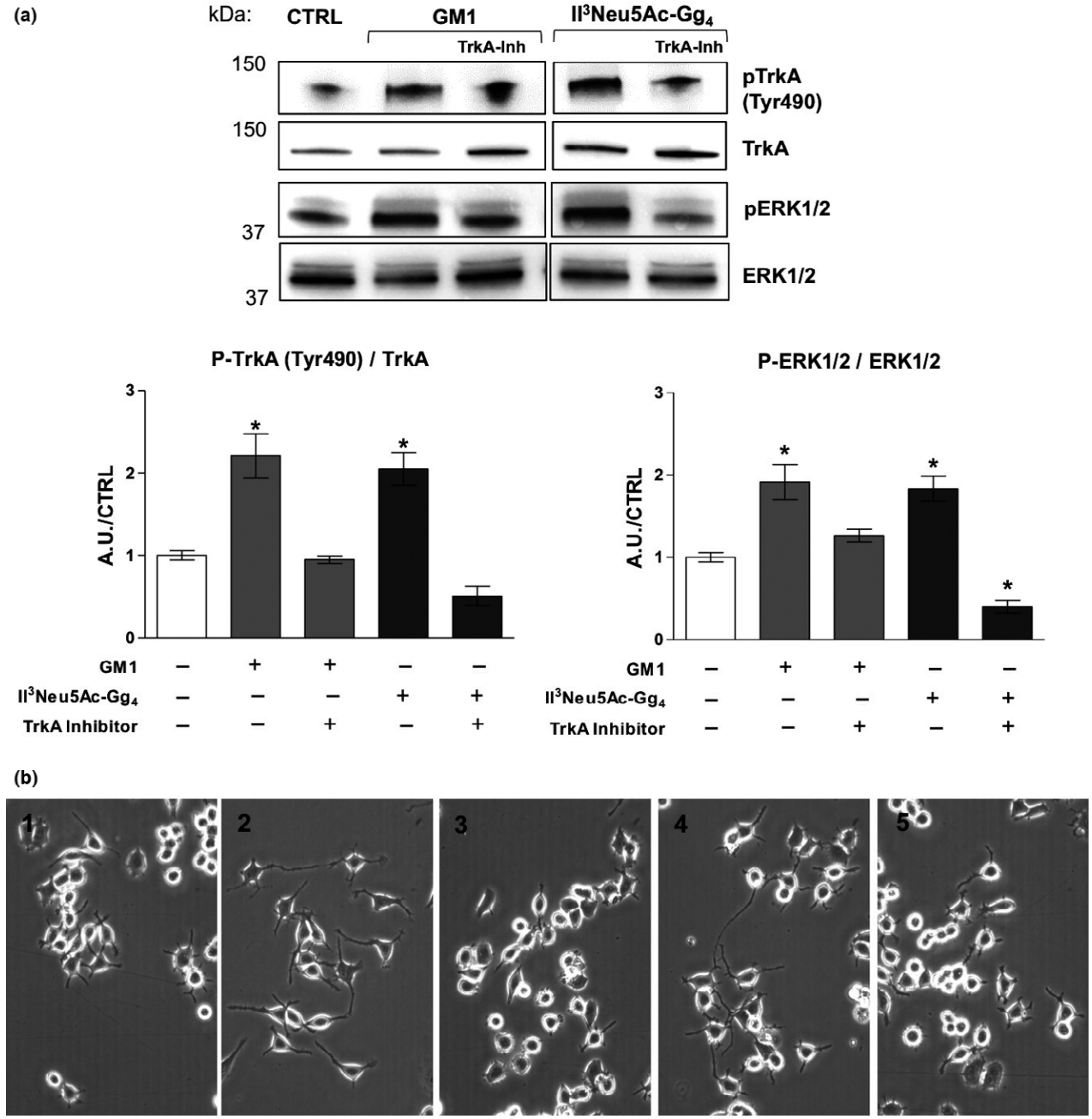

Fig. 6 GM1 and II^{3}Neu5Ac-Gg$_4$ effect on TrkA pathway. Neuro2a (N2a) cells were treated with 50 μM GM1 and II^{3}Neu5Ac-Gg$_4$ for 24 h. Where indicated, the TrkA receptor inhibitor (120 nM) was added to the N2a cells as mentioned in Methods section. (a) Expression of TrkA, phosphorylated TrkA (tyrosine 490, Tyr490), total extracellular signal-regulated protein kinases 1 and 2 (ERK1/2) and phosphorylated ERK1/2 in cell lysate by means of specific antibodies and revealed by enhanced chemiluminescence. Top: immunoblotting images are shown. Bottom: Semi-quantitative analysis of phosphorylated TrkA and ERK1/2 related to total level of TrkA and ERK 1/2, respectively. Data are expressed as fold increase over control of the mean ± SEM from five different experiments (*$p < 0.05$, Student's *t*-test, $n = 5$). (b) Morphological analysis of N2a cells. 1, control; 2, GM1; 3, TrkA-Inh + GM1; 4, II^{3}Neu5Ac-Gg$_4$; 5: TrkA-Inh + II^{3}Neu5Ac-Gg$_4$. Following 24 h incubation, cells were evaluated with phase contrast microscopy with 200× magnification. Images are representative of ten independent experiments ($n = 10$).

In fact, residues of the total structure, such as sialic acid, galactose, sialyllactose, Neu5Ac-Gg$_3$ and Gg$_4$, did not show neuritogenic properties, at least at the used concentration (Fig. 3 and Figure S1). On the other hand, fucosylated II^{3}Neu5Ac-Gg$_4$ showed the same effect of II^{3}Neu5Ac-Gg$_4$ suggesting that the terminal α-Fuc-(1-2)-β-Gal linkage does not change the conformation of the Neu5Ac-Gg$_4$ necessary for the activation of the sprouting process (Fig. 3 and

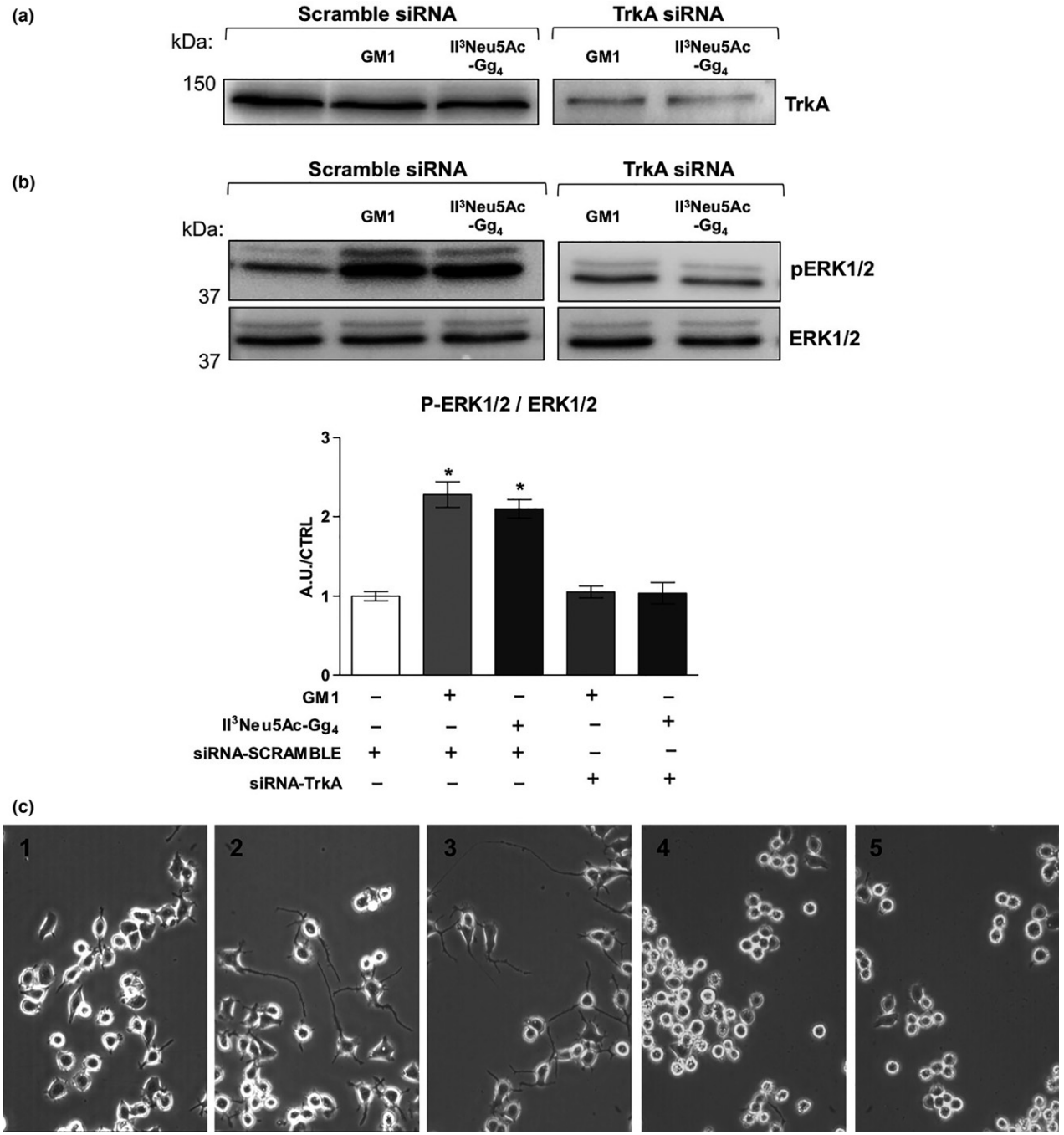

Fig. 7 Effect of GM1 and II^{3}Neu5Ac-Gg$_4$ on Neuro2a (N2a) cells following silencing of TrkA. N2a cells were transfected with siRNA against TrkA (50 nM) as described in Methods section. Control cells were transfected with scramble-siRNA. 24 h after transfection cells were exposed to 50 μM GM1 or II^{3}Neu5Ac-Gg$_4$ for 24 h. (a) Western blotting representative image for TrkA expression in siRNA treated cells. (b) Expression of total extracellular signal-regulated protein kinases 1 and 2 (ERK1/2) and phosphorylated ERK1/2 by specific antibodies and revealed by enhanced chemiluminescence. Top: representative immunoblotting images. Bottom: Semi-quantitative analysis of phosphorylated ERK1/2 related to ERK 1/2 total level. Data are expressed as fold increase over control of the mean ± SEM from five different experiments (*$p < 0.05$, Student's *t*-test, $n = 5$). (c) Morphological analysis of N2a cells 1, scramble-siRNA; 2, scramble-siRNA + GM1; 3, scramble-siRNA + II^{3}Neu5Ac-Gg$_4$; 4, siRNA-TrkA + GM1; 5, siRNA-TrkA + II^{3}Neu5Ac-Gg$_4$. Following 24 h incubation, cells were evaluated with phase contrast microscopy with 200× magnification. Images are representative of ten independent experiments ($n = 10$).

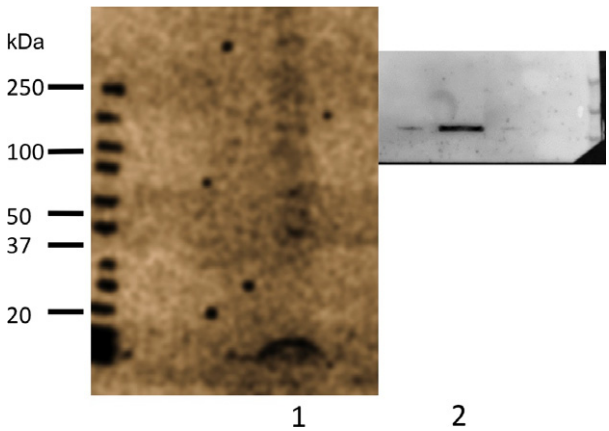

Fig. 8 Interaction between TrkA and II^{3}Neu5Ac-Gg$_4$ in Neuro2a (N2a) cells. Photoactivable II^{3}Neu5Ac-[^{3}H]Gg$_4$-N$_3$ was added to N2a cells and cells were then illuminated. Cell lysate was submitted to 4–20% sodium dodecyl sulfate–polyacrylamide gel electrophoresis, blotted on a polyvinylidene difluoride (PVDF) membrane and visualized by digital autoradiography for 96 h (lane 1). The same PVDF was visualized by western blotting using specific antibody anti-TrkA (lane 2). The image is representative of three different experiments.

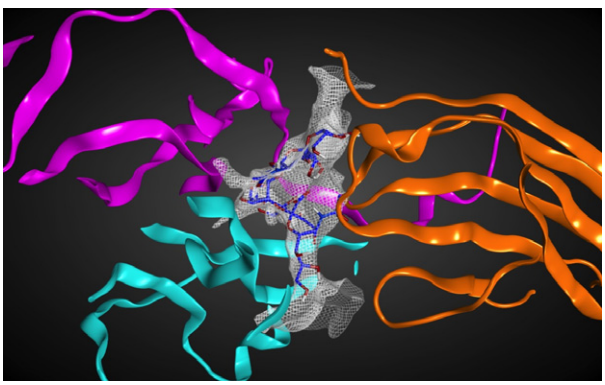

Fig. 9 Molecular dynamic calculations for the complex TrkA–nerve growth factor (NGF)–II^{3}Neu5AcGg$_4$. Top-scoring docking pose of II^{3}Neu5Ac-Gg$_4$ in the TrkA-NGF crystallographic complex. TrkA in orange ribbons; two NGF molecules: one in cyan ribbons and one in magenta ribbons. II^{3}Neu5AcGg$_4$ is represented in sticks, with blue color for carbon atoms and red color for oxygen atoms. Van der Waals interaction surface between II^{3}Neu5AcGg$_4$ and proteins is represented as a white mesh map.

Figure S1). This evidence agrees with the previous information reporting that GM1 and Fuc-GM1 show similar binding constant for cholera toxin (Masserini *et al.* 1992).

It has been reported that nerve growth factor receptor TrkA requires the presence of GM1-enriched membrane to be active, while the absence of ganglioside GM1 is negatively correlated with TrkA function (Ferrari *et al.* 1995; Mutoh *et al.* 1995, 1998; Farooqui *et al.* 1997; Rodriguez *et al.* 2001; Bachis *et al.* 2002; Da Silva *et al.* 2005). TrkA phosphorylation at Tyr490 residue induces the phosphorylation cascade as shown in Fig. 10 (Huang and Reichardt 2003; Brodeur *et al.* 2009). Previous finding revealed the activation of the TrkA-Erk1/2 pathway by ganglioside GM1 (Farooqui *et al.* 1997; Singleton *et al.* 2000; Duchemin *et al.* 2002; Zakharova *et al.* 2014). Thus, we studied the TrkA-Erk1/2 pathway following the addition of II^{3}Neu5Ac-Gg$_4$ to N2a. For the first time, we showed that, II^{3}Neu5Ac-Gg$_4$ enhances the phosphorylation of Tyr490 of TrkA and of Erk1/2 leading to neurodifferentiation (Fig. 6). To confirm that the GM1–TrkA interaction triggers the differentiation, we silenced or inhibited TrkA. In both experiments, the addition of II^{3}Neu5Ac-Gg$_4$ to the cells did not promote neurite sprouting nor reduced the cell proliferation (Figs 6 and 7).

These findings support that the well-known GM1 neurotrophic effects are mediated by TrkA receptor, which could be considered an II^{3}Neu5Ac-Gg$_4$ target.

To obtain evidence about the formation of an II^{3}Neu5Ac-Gg$_4$-TrkA complex, we prepared a tritium-labeled photoactivable II^{3}Neu5Ac-Gg$_4$ by chemical techniques (Fig. 1). Photolabeling experiments with photoactivable glycosphingolipids were introduced several years ago (Loberto *et al.* 2003; Mauri *et al.* 2004) and were used to ascertain the interaction of glycosphingolipids with different proteins, such as the insulin receptor (Kabayama *et al.* 2007), the receptor CD9 (Ono *et al.* 2001), the cytoskeleton tubulin (Palestini *et al.* 2000), the membrane protein caveolin 1 (Fra *et al.* 1995), the kinase Lyn (Chiricozzi *et al.* 2015), and the neuronal protein TAG1 (Loberto *et al.* 2003).

After incubation with the tritium-labeled photoactivable II^{3}Neu5Ac-Gg$_4$, cells were washed once with PBS to remove the non-cell-associated compound. The subsequent UV-light exposition transforms the photoactivable group into a nitrene, which rapidly covalently links to neighboring compounds (Mauri *et al.* 2004). According to this mechanism, and recalling that the exogenous II^{3}Neu5Ac-Gg$_4$ does not become component of the cell membranes, any interaction of the tritium-labeled II^{3}Neu5Ac-Gg$_4$ photoactivable derivative with proteins yields to tritium-labeled II^{3}Neu5Ac-Gg$_4$-protein stable complexes that should involve the extracellular domain of transmembrane proteins or of GPI-anchored proteins. By SDS–PAGE separation, followed by radioimaging of the blotted material, we recognized few bands and one of these bands showed a molecular mass of 140 KDa. A specific signal for TrkA was found overlapping the radiolabeled band, suggesting a direct interaction between II^{3}Neu5Ac-Gg$_4$ and TrkA (Fig. 8).

Over these experimental data, we used molecular modeling tools to predict whether II^{3}Neu5Ac-Gg$_4$ can increase the TrkA-NGF complex stability, favoring their intermolecular interactions. In fact, even if NGF is not synthetized by N2a cells (Leon *et al.* 1994), it is present in our experimental conditions since the culture medium used contains serum (Figure S3). We started from the crystallized structure of

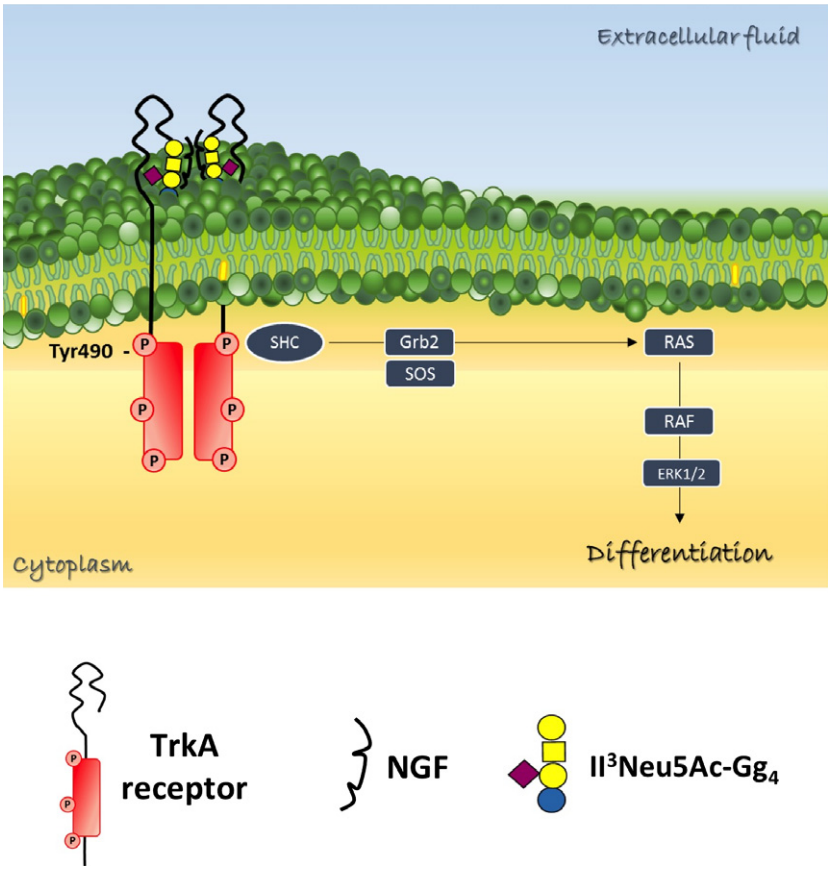

Fig. 10 Diagram of the proposed mechanism for GM1-mediated neurodifferentiation in Neuro2a cells. The TrkA activation by autophosphorylation is regulated by GM1-enriched receptor environment. GM1 modulates TrkA activity by stabilizing the TrkA-nerve growth factor (NGF) complex with its oligosaccharide portion. The TrkA-GM1 interaction is represented as a side-by-side interaction. GM1 triggers the phosphorylation of Tyr490 promoting the differentiation signaling. ERK, extracellular signal-regulated protein kinases 1 and 2; Grb2, growth factor receptor-bound protein 2; Gab1, Grb2-associated binder-1; RAS, GTP-binding protein; RAF, serine/threonine kinase; SHC, transforming protein 1; SOS, son of sevenless.

TrkA receptor, which is resolved as a dimer in the presence of NGF. The crystal structure of the TrkA-NGF complex is characterized by a pocket, which can be occupied by water molecules, as showed in another crystallographic structure of the same complex (PDB ID: 1WWW). By *in silico* analysis, we found that the $II^3Neu5Ac\text{-}Gg_4$ perfectly fits within this space (Fig. 9). Moreover, the energy associated to the TrkA–$II^3Neu5Ac\text{-}Gg_4$ complex, approx. −6.6 kcal/mol, becomes approx. −11.5 kcal/mol when NFG belongs to the complex. This suggests that the $II^3Neu5Ac\text{-}Gg_4$ stabilizes the TrkA–NGF interaction, and suggests a specific molecular recognition process between the $II^3Neu5Ac\text{-}Gg_4$ and a specific extracellular domain of the TrkA receptor.

The information available in literature clearly shows that any experimental model capable to modify the local plasma membrane GM1 content, promotes N2a differentiation. GM1 is a natural amphiphilic compound with a structure that combines the ceramide lipid moiety with the soluble oligosaccharide chain. Altogether, our results point out that the GM1 oligosaccharide is the structure portion responsible for the neurodifferentiative properties exerted by GM1 (Fig. 10). The GM1 oligosaccharide directly interacts with TrkA receptor resulting in TrkA-mediated neuritogenesis.

Neuronal differentiation is characterized by an enhancement of several glycosyltransferases activity leading to an increase in PM ganglioside content (Aureli *et al.* 2011). Ceramide is the aglycone necessary for glycan protrusion into the extracellular environment and for interaction with functional proteins. GM1 exhibits its oligosaccharide chain to the TrkA receptor. Molecular dynamic calculations confirm that the GM1 oligosaccharide perfectly fits with a TrkA domain stabilizing the TrkA–NGF interaction, allowing a rapid auto phosphorylation of the receptor cytosolic portion.

The still open question is whether the $II^3Neu5Ac\text{-}Gg_4$–TrkA interaction is due to a broad plasma membrane increase of GM1 or to a membrane reorganization, leading to a new TrkA environment enriched of GM1. We reported this latter possibility because silencing plasma membrane sialidase Neu3, with consequent less hydrolysis of polysialylated gangliosides and with reduced production of GM1 at the plasma membrane level, we promoted the neurite elongation (Valperta *et al.* 2007). We discussed this in term of membrane reorganization and local concentration of GM1.

Acknowledgments and conflict of interest disclosure

This work was supported by the 2015–2016 contract from FIDIA S.p.a. in favor of S.S. The authors declare that they have no conflict of interest.

Supporting information

Additional Supporting Information may be found online in the supporting information tab for this article:

Figure S1. This figure shows the morphological characterization of N2a cells untreated or treated with GM1, $II^3Neu5Ac\text{-}Gg_4$, and saccharide derivative for 48 h.

Figure S2. This figure shows the MS and chromatography analysis of $II^3Neu5Ac\text{-}Gg_4$.

Figure S3. This figure shows the evaluation of NGF expression in N2a cells.

Appendix S1. Supplementary Materials and methods.

References

Acquotti D., Cantu L., Ragg E. and Sonnino S. (1994) Geometrical and conformational properties of ganglioside GalNAc-GD1a, $IV^4GalNAcIV^3Neu5AcII^3Neu5AcGgOse_4Cer$. *Eur. J. Biochem.* **225**, 271–288.

Allende M. L. and Panzetta P. (1994) *In vitro* modulation of changes inganglioside patterns of differentiating neurons in the presence of ananti-GM1 antibody. *J. Neurosci. Res.* **37**, 497–505.

Aureli M., Loberto N., Lanteri P., Chigorno V., Prinetti A. and Sonnino S. (2011) Cell surface sphingolipid glycohydrolases in neuronal differentiation and aging in culture. *J. Neurochem.* **116**, 891–899.

Aureli M., Mauri L., Ciampa M. G., Prinetti A., Toffano G., Secchieri C. and Sonnino S. (2016) GM1 ganglioside: past studies and future potential. *Mol. Neurobiol.* **53**, 1824–1842.

Bachis A., Rabin S. J., Del Fiacco M. and Mocchetti I. (2002) Ganglioside prevent excitotoxicity trought activation of TrkB receptor. *Neurotox. Res.* **4**, 225–234.

Brodeur G. M., Minturn J. E., Ho R., Simpson A. M., Iyer R., Varela C. R., Light J. E., Kolla V. and Evans A. E. (2009) Trk receptor expression and inhibition in neuroblastoma. *Clin. Cancer Res.* **15**, 3244–3250.

Chigorno V., Pitto M., Cardace G., Acquotti D., Kirschner G., Sonnino S., Ghidoni R. and Tettamanti G. (1985) Association of ganglio-sides to fibroblasts in culture: a study performed with GM1 [14C]-labelled at the sialic acid acetyl group. *Glycoco. J.* **2**, 279–291.

Chigorno V., Valsecchi M., Acquotti D., Sonnino S. and Tettamanti G. (1990) Formation of cytosolic ganglioside-protein complex following administration of photoreactive ganglioside GM1 to human fibroblasts in culture. *FEBS Lett.* **263**, 329–331.

Chiricozzi E., Ciampa M. G., Brasile G., Compostella F., Prinetti A., Nakayama H., Ekyalongo R. C., Iwabuchi K., Sonnino S. and Mauri L. (2015) Direct interaction, instrumental for signaling processes, between LacCer and Lyn in the lipid rafts of neutrophil-like cells. *J. Lip. Res.* **56**, 129–141.

Coskun U. and Simons K. (2011) Cell membranes: the lipid perspective. *Cell Struct.* **19**, 1543–1548.

Da Silva J. S., Hasegawa T., Miyagi T., Dotti C. G. and Abab-Rodriguez J. (2005) Asymmetric membrane ganglioside sialidase activity specifies axonal fate. *Nat. Neurosci.* **8**, 606–615.

Duchemin A. M., Ren Q., Mo L., Neff N. H. and Hadjiconstantinou M. (2002) GM1 ganglioside induces phosphorylation and activation of Trk and Erk in brain. *J. Neurochem.* **81**, 696–707.

Facci L., Leon A., Tofffano G., Sonnino S., Ghidoni R. and Tettamanti G. (1984) Promotion of neuritogenesis in mouse neuroblastoma cells by exogenous gangliosides. Relationship between the effect and the cell association of ganglioside GM1. *J. Neurochem.* **42**, 299–305.

Farooqui T., Franklin T., Pearl D. K. and Yates A. J. (1997) Ganglioside GM1 enhances induction by nerve growth factor of a putative dimer of TrkA. *J. Neurochem.* **68**, 2348–2355.

Ferrari G., Anderson B. L., Stephens R. M., Kaplan D. R. and Greene L. A. (1995) Prevention of apoptotic neuronal death by GM1 ganglioside. Involvement of Trk neurotrophin receptors. *J. Biol. Chem.* **270**, 3074–3080.

Fra A. M., Masserini M., Palestini P., Sonnino S. and Simons K. (1995) A photo-reactive derivate of ganglioside GM1 specifically cross-links VIP21-caveolin on the cell surface. *FEBS Lett.* **375**, 11–14.

Fukuda Y., Fukui T., Hikichi C. *et al.* (2014) Neurotrophin promotes NGF signaling through interaction of GM1 ganglioside with Trk neurotrophin receptor in PC12 cells. *Brain Res.* **1596**, 13–21.

Ghidoni R., Sonnino S., Tettamanti G., Wiegandt H. and Zambotti V. (1976) On the structure of two new gangliosides from beef brain. *J. Neurochem.* **27**, 511–515.

Hakomori S., Handa K., Iwabuchi K., Yamamura S. and Prinetti A. (1998) New insights in glycosphingolipid function: 'glycosignaling domain', a cell surface assembly of glycosphingolipids with signaltransducer molecules, involved in cell adhesion coupled with signaling. *Glycobiology* **8**, xi–xix.

Huang E. J. and Reichardt L. F. (2003) Trk receptors: roles in neuronal signal transduction. *Ann. Rev. Biochem.* **72**, 609–642.

IUPAC-IUBMB JCoBN, (1998) Nomenclature of glycolipids. *Carbohydr Res* **312**, 167–175.

Kabayama K., Sato T., Saito K., Loberto N., Prinetti A., Sonnino S., Kinjo M., Igarashi Y. and Inokuchi J. (2007) Dissociation of the insulin receptor and caveolin-1 complex by ganglioside GM3 in the state of insulin resistance. *Proc. Natl Acad. Sci. USA* **104**, 13678–13683.

Kuhn R. and Wiegandt H. (1963) Die Konstitution der Ganglio-N-tetraose und des Gangliosids. *GI Chem. Ber.* **96**, 866–880.

Kwak D. H., Kim S. M., Lee D. H., Kim J. S., Kim S. M., Lee S. U., Jung K. Y., Seo B. B. and Choo Y. K. (2005) Differential expression patterns of gangliosides in the ischemic cerebral cortexproduced by middle cerebral artery occlusion. *Mol. Cell* **20**, 354–360.

Ledeen R. W. and Wu G. (2015) The multi-tasked life of GM1 ganglioside, a true factotum of nature. *Trends Biochem. Sci.* **40**, 407–418.

Leon A., Buiuani A., Dal Toso R., Fabris M., Romanello S., Aloeo L. and Montalcini R. L. (1994) Mast cells synthesize, store, and release nerve growth factor. *Proc. Natl Acad. Sci. USA* **91**, 3739–3743.

Lipartiti M., Lazzaro A., Zanoni R., Mazzari S., Toffano G. and Leon A. (1991) Monosialoganglioside GM1 reduces NMDA neurotoxicity in neonatal rat brain. *Exp. Neurol.* **113**, 301–305.

Loberto N., Prioni S., Prinetti A., Ottico E., Chigorno V., Karagogeos D. and Sonnino S. (2003) The adhesion protein TAG-1 has a ganglioside environment in the sphingolipid-enriched membran domains of neuronal cell in culture. *J. Neurochem.* **85**, 224–233.

Lubineau A., Auge J. and Drouillat B. (1995) Improved synthesis of glycosylamines and a straightforward preparation of N-acylglycosylamines as carbohydrate-based detergents. *Carbohydr. Res.* **266**, 211–219.

Masserini M., Freire E., Palestini P., Calappi E. and Tettamanti G. (1992) Fuc-GM1 ganglioside mimics the receptor function of GM1 for cholera toxin. *Biochemistry* **31**, 2422–2426.

Mauri L., Prioni S., Loberto N., Chigorno V., Prinetti A. and Sonnino S. (2004) Synthesis of radioactive and photoactivable ganglioside derivates for the study of ganglioside-protein interaction. *Glycoconj. J.* **20**, 11–23.

Mehlen P., Rabizadeh S., Snipas S. J., Assa-Munt N., Salvesen G. S. and Bredesen D. E. (1988) The DCC gene product induces apoptosis by a mechanism requiring receptor proteolysis. *Nature* **395**, 801–804.

Miyagi T. and Yamaguchi K. (2012) Mammalian sialidases: physiological and pathological roles in cellular functions. *Glycobiology* **22**, 880–896.

Mocchetti I. (2005) Exogenous gangliosides, neuronal plasticity and repair and the nurotrophins. *Cell. Mol. Life Sci.* **62**, 2283–2294.

Mosmann T. (1983) Rapid colorimetric assay for cellular growth and survival: application to proliferation and cytotoxicity assays. *J. Immunol. Methods* **65**, 55–63.

Mutoh T., Tokuda A., Miyadai T., Hamaguchi M. and Fujiki N. (1995) Ganglioside GM1 binds to the Trk proteins and regulates receptor function. *Proc. Natl Acad. Sci.* **92**, 5087–5091.

Mutoh T., Tokuda A., Inokuchi J. and Kuriyama M. (1998) Glucosylceramide synthase inhibitor inhibits the action of nerve growth factor in PC12 cells. *J. Biol. Chem.* **273**, 26001–26007.

Naim M., Bhat S., Rankin K. N. *et al.* (2007) Solvated interaction energy (SIE) for scoring protein-ligan binding affinities. 1. Exlporing the parameter space. *J. Chem. Inf. Model.* **47**, 122–133.

Ono M., Handa K., Sonnino S., Withers D. A., Nagai H. and Hakomori S. (2001) GM3 ganglioside inhibits CD9-facilitated haptotactic cell motility: coexpression of GM3 and CD9 is essential in the downregulation of tumor cell motility and malignancy. *Biochemistry* **40**, 6414–6421.

Palestini P., Pitto M., Tedeschi G., Ferraretto A., Parenti M., Brunner J. and Masserini M. (2000) Tubulin anchoring to glycolipid-enriched, detergent resistent domains of the neuronal plasma membrane. *J. Biol. Chem.* **275**, 9978–9985.

Rabin S. J., Bachis A. and Mocchetti I. (2002) Gangliosides activate Trk receptors by inducing the release of neurotrophin. *J. Biol. Chem.* **51**, 49466–49472.

Rodriguez J. A., Piddini E., Hasegawa T., Miyagi T. and Dotti C. G. (2001) Plasma membrane ganglioside sialidase regulates axonal growth and regeneration in hippocampal neurons in culture. *J. Neurosci.* **21**, 8387–8395.

Roisen F. J., Bartfeld H., Nagele R. and Yorke G. (1981) Ganglioside stimulation of axonal sprouting in vitro. *Science* **214**, 577–578.

Schengrund C. L. (2015) Gangliosides: glycosphingolipids essential for normal neural development and function. *Trends Biochem. Sci.* **40**, 397–406.

Schengrund C. L. and Prouty C. (1988) Oligosaccharide portion of GM1 enhances process formation by S20Y neuroblastoma cells. *J. Neurochem.* **51**, 277–282.

Schneider J. S., Sendek S., Daskalakis C. and Cambi F. (2010) GM1 ganglioside in Parkinson's disease: results of five year open study. *J. Neurol. Sci.* **292**, 45–51.

Singleton D. W., Lu C. L., Collela R. and Roisen F. J. (2000) Promotion of neurite outgrowh by protein kinase inhibitors and ganglioside GM1 in neuroblastoma cells involved MAP kinase ERK1/2. *Int. J. Dev. Neurosci.* **18**, 797–805.

Sonnino S., Chigorno V., Acquotti D., Pitto M., Kirschner G. and Tettamanti G. (1989) A photoreactive derivative of radiolabeled GM1 ganglioside: preparation and use to establish the involvment of specific proteins in GM1 uptake by human fibroblasts in culture. *Biochemistry* **28**, 77–84.

Sonnino S., Chigorno V., Valsecchi M., Pitto M. and Tettamanti G. (1992) Specific ganglioside-cell protein interactions: a study performed with GM1 ganglioside derivative containing photoactivable azide and rat cerebellar granule cells in culture. *Neurochem. Int.* **20**, 315–321.

Sonnino S., Nicolini M. and Chigorno V. (1996) Preparation of radiolabeled gangliosides. *Glycobiology* **6**, 479–487.

Sonnino S., Mauri L., Chigorno V. and Prinetti A. (2006) Gangliosides as components of lipid membrane domains. *Glycobiology* **17**, 1R–13R.

Sonnino S., Chigorno V., Aureli M., Masilamani A. P., Valsecchi M., Loberto N., Prioni S., Mauri L. and Prinetti A. (2011) Role of gangliosides and plasma membrane associated sialidase in the process of cell membrane organization. *Adv. Exp. Med. Biol.* **705**, 297–316.

Svennerholm L. (1957) Quantitative estimation of sialic acids II A colorimetric resorcinol hydrochloric acid method. *Biochim. Biophys. Acta* **24**, 604–611.

Takki-Luukkainen I. T. and Miettinen T. (1959) Presence of sialic acid and hexosamine in proteins of the aqueous humour. *Acta Ophthalmol.* **37**, 138–142.

Tettamanti G. (1986) *Gangliosides and Neuronal Plasticity*. Meeting ISfN. Liviana Press, Springer, Verlag, Paris, France.

Tettamanti G., Bonali F., Marchesini S. and Zambotti V. (1973) A new procedure for the extraction, purification and fractionation of brain gangliosides. *Biochim. Biophys. Acta* **296**, 160–170.

Valperta R., Valsecchi M., Rocchetta F., Aureli M., Prioni S., Prinetti A., Chigorno V. and Sonnino S. (2007) Induction of axonal differentiation by silencing plasma membrane-associated sialidase Neu3 in neuroblastoma cells. *J. Neurochem.* **100**, 708–719.

Wiegandt H. and Bucking H. W. (1970) Carbohydrate components of extraneuronal gangliosides from bovine and human spleen, and bovine kidney. *Eur. J. Biochem.* **15**, 287–292.

Wood E. R., Kuyper L., Petrov K. G., Hunter R. N., Harris P. A. and Lackey K. (2004) Discovery and in vitro evaluation of potent TrkA kinase inhibitors: oxindole and aza-oxindoles. *Bioorg. Med. Chem. Lett.* **14**, 953–957.

Wu G., Lu Z. H. and Ledeen R. W. (1995) Induced and spontaneous neuritogenesis are associated with enhanced expression of ganglioside GM1 in the nuclear membrane. *J. Neurosci.* **15**, 3739–3746.

Yu R. K., Nakatani Y. and Yanagisawa M. (2009) The role of glycosphingolipid metabolism in the developing brain. *J. Lipid Res.* **50**, S440–S445.

Zakharova I. O., Sokolova T. V., Vlasova Y. A., Furaev V. V., Rychkova M. P. and Avrova N. F. (2014) GM1 ganglioside activates ERK1/2 and Akt downstream of Trk tyrosine kinase and protects PC12 cell against hydrogen peroxide toxicity. *Neurochem. Res.* **39**, 2262–2275.

Zoli M., Benfanti F., Pich E. M., Toffano G., Fuxe K. and Agnati L. F. (1990) Aspects of neuronal plasticity in the central nervous system – IV. Chemical anatomical studies on the aging brain. *Neurochem. Int.* **16**, 437–449.

